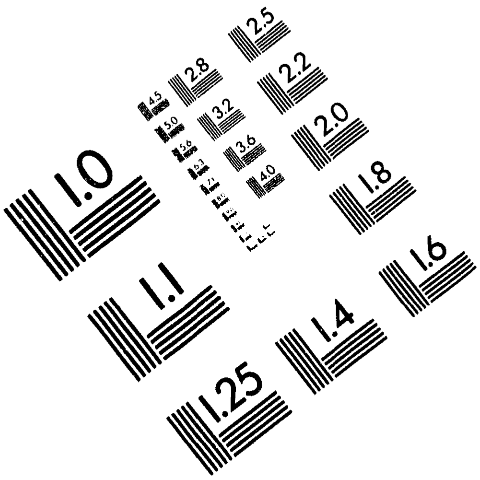

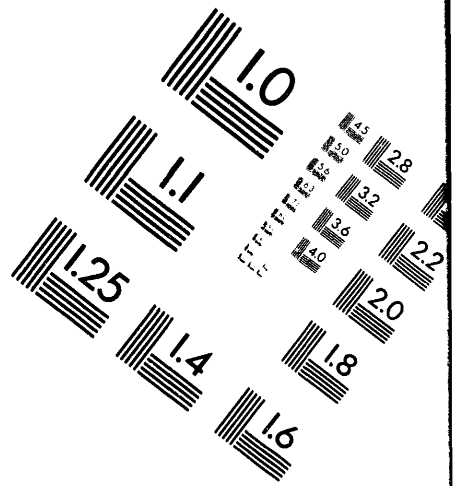

Association for Information and Image Management
1100 Wayne Avenue, Suite 1100
Silver Spring, Maryland 20910
301/587-8202

Centimeter

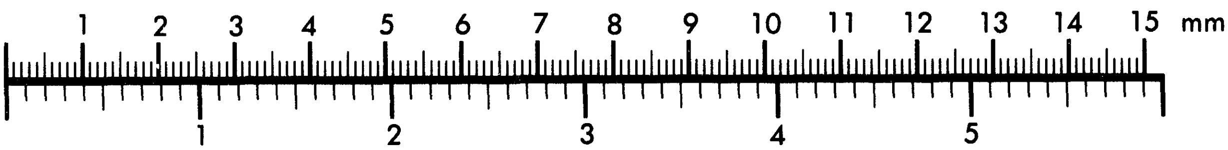

Inches

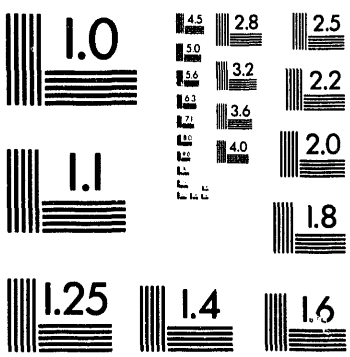

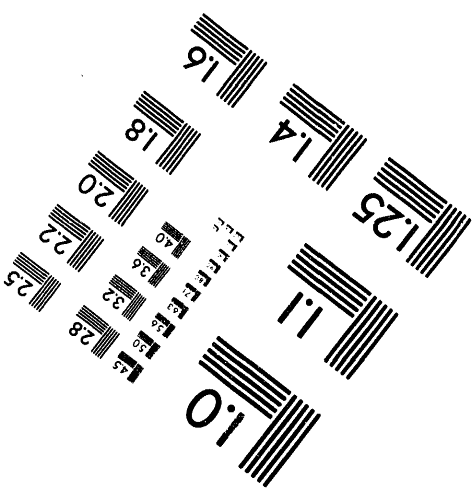

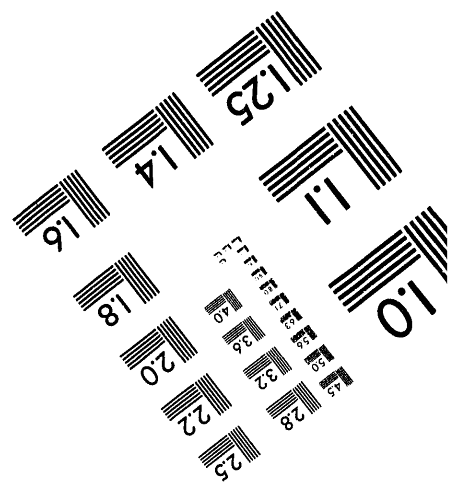

1 of 1

A 250 GHz Microwave Interferometer for Divertor Experiments on DIII-D

R.A. James, D.G. Nilson, R.D. Stever and D.N. Hill, T.A. Casper

Lawrence Livermore National Laboratory, University of California, Livermore, California 94551

(Presented on 9 May 1994)

Abstract:

A new 250 GHz, two-frequency microwave interferometer system has been developed to diagnose divertor plasmas on DIII-D. This diagnostic will measure the line-averaged density across both the inner and outer, lower divertor legs. With a cut-off density of over 7×10^{14} cm^{-3}, temporal measurements of ELMs, MARFs and plasma detachment are expected. The outer leg system will use a double pass method while the inner leg system will be single pass. Two special 3D carbon composite tiles are used, one to protect the microwave antennas mounted directly under the strike point and the other as the outer leg reflecting surface. Performance, design constraints, and the thermal-mechanical design of the 3D carbon composite tiles are discussed.

Introduction:

A microwave interferometer operating in the 1mm range has been designed and installed on the DIII-D tokamak. The purpose of this instrument is to make simultaneous measurements of the line averaged density across both the inner and outer, lower divertor legs. Due to the interferometer's physical location and its operating frequency, several constraints have influenced the design. From the microwave standpoint, these include minimizing the transmission losses and accommodating refraction. For the mechanical design, large thermal stresses caused by the divertor heat flux required the use of protective tiles composed of 3D carbon composite material (1).

I. Principles of Interferometery

By passing an electromagnetic wave through a plasma column, a phase shift related to the line averaged electron density develops on the emerging wave (2,3). In short, for a two-arm interferometer operating with O-mode polarization (E parallel to B), the phase difference between the plasma and reference arms becomes (in cgs units):

$$\Delta\emptyset = (8.45\text{x}10^{-3}/f) \int n_e(z)\, dz \qquad \text{(radians)} \quad \text{equ.1}$$

where f is the probe wave frequency and the integral is along the path through the plasma. The phase difference can also expressed in fringes: $F=\Delta\emptyset/2\pi$. In order to transit the plasma, the probing wave must have a frequency f greater than the electron plasma frequency, f_{pe}. For O-mode polarization this criteria establishes the cut-off density n_{co}, an upper bound on the measurable plasma density; $n_e < n_{co} = 1.23\text{x}10^{-8}$ f^2 cm^{-3}.

II. Mechanical Layout

A. General Layout

Figure 1 diagrams the general layout for the diagnostic. Beginning at the microwave chassis, microwaves at two operating frequencies (f1,f2) are routed inside the DIII-D vessel and launched from a V-1 port in the lower divertor floor. The outer divertor leg uses a double pass system while the inner leg is a single pass system.

For the inner divertor leg system, the transmitted signal is captured by an antenna located behind the inner wall tiles and views the V-1 port through a 2.5cm hole. The signal returns to the V-1 port using waveguide underneath the vessel tiles. For the outer divertor leg, a mirror surface is cut at an angle into the surface of a bias ring tile and the reflected signal is captured by an antenna in the V-1 port. Both signals are routed back to the microwave chassis where they are detected using a microwave receiver. The two plasma phase signals as well as their corresponding reference signals are beat down to 30 MHz and shipped to the Control Room Annex using fiber optic cables. The net plasma phase is determined using digital phase comparators capable of measuring up to 16 fringes with an accuracy of 1/100th of a fringe. The signals are then digitized at 5kHz and acquired by the data acquisition computer.

B. Microwave Transport Details

All of the waveguide runs to and from the microwave chassis are composed of WR28 rectangular copper waveguide (0.356 x 0.711 cm). An external dc break composed of 0.005 cm thick mylar is used. The launching and receiving antennas are open-ended WR28 waveguide and flat sub-mirror reflectors, see Fig. 2. In routing the transmitted signal from the inside wall back to the V-1 port three H-plane bends are used; two 45° radius (r=12.7cm) bends and one 90° miter bend. Externally, four H-plane miter bends are used, one for each waveguide run.

The vacuum interface for the microwave waveguides is composed of Viton O-rings and fused quartz windows (n=1.96), each with a thickness of 0.12cm; $2\lambda_q$ @ 250GHz. To minimize mode conversion at this interface, the inside edges of the waveguides are beveled and the waveguide-window separation is minimized; less than 0.24cm or $2\lambda_v$.

In order to minimize the lengths of the overmoded waveguide runs, the microwave chassis, its power supply and the fiber optic transmitters are all located directly below the port. From the vessel floor to the microwave chassis, each waveguide run is ≈400cm long. The inside wall waveguide run adds ≈75cm to that run. To prevent the waveguide runs from bending and twisting during machine baking and disruptions, the internal vertical runs are captured in channels cut into a square stainless steel bar which runs the length of the V-1 vacuum

port, ≈180cm. Magnetic shielding is provided by an iron box (35x35x40cm) with 1.9cm thick walls, which reduces the magnetic field from the Ohmic coil to less than 5 Gauss inside the box.

III. Bias Ring and Floor Tile Design

A finite element stress analysis code (ANSYS 5.0) was used to predict the thermal stresses expected as a result of the modifications to two of the vessel's protective tiles; a bias ring tile and a divertor floor tile. The analysis used 3D carbon composite material (1) and a heating profile (radiative and particle) determined by IR camera analysis (4) with a peak heat load of 620 W/cm^2 for 5 seconds, characteristic of a 12.8MW neutral beam discharge. Properties for the 3D carbon were obtained from a McDonnell Douglas test report (5).

Tile modifications include a 7.5cm diameter tapered hole, centered in the middle of a floor tile and a reflecting surface cut at an angle into a bias ring tile. For the floor tile, the vertical cross section of the tapered hole is such that a field line with an angle of incidence greater than 8° (edge q<3) is required to directly hit any of the microwave hardware located in its bore, see Fig. 2. In the case of the bias ring tile, the mirror surface is aligned perpendicular to the microwave antennas in the V-1 port and the remainder of this surface is gradually tapered back to the edge, see Fig. 3b.

For both tiles, the contoured surfaces lead to a 1.5 to 3 fold increase of the heat flux on portions of the remaining tile surface, i.e. the heat load which would have been intercepted by the uncut surfaces is now absorbed by another segment of the tile. In Fig. 3, the stress profile for both modified tiles is shown.

The predicted maximum compressive and tensile stresses for both tiles are below the maximum rating (125 MPA (-) and 147 MPA (+) @ 982°C) for the 3D carbon composite material. For the bias ring tile, the predicted stresses are 101 MPA and 34 MPA respectively and for the floor tile the predicted stresses are 83 MPA and 37 MPA respectively.

IV. Microwave system

A. Microwave Transmitter, Receiver and Antenna Design

In Fig. 4, a schematic of the microwave system is shown. The generation of 1mm microwaves for the two transmitters (f1,f2) is accomplished using Gunn oscillators and waveguide triplers. For the receiver, W-band mixers have been optimized for 3rd harmonic conversion. For both the plasma and reference arm receivers' only one mixer is used. For the plasma arm, the two return lines from the machine are combined in fundamental waveguide (WR4) using a hybrid tee. For the reference arm, signals from WR8 sidewall couplers are combined using a H-plane magic tee.

Widely spaced IFs, 4.2 and 5.0GHz are beat down to 30MHz using voltage tunable (4-8 GHz) local oscillators (f4, f5). These oscillators are locked to any frequency drift in f1 and f2 using the phase detection circuitry in the reference arm's IF section. Body heaters on f1 and f2 limit their frequency drift to less than ±20MHz. A second phase detection circuit operates to frequency lock f3 using a 7.225 GHz local oscillator, a harmonic mixer (n=12) and a 300 MHz crystal oscillator.

Design of the antenna patterns required a trade-off between signal strength and flexibility needed because of refraction. Due to their easier mechanical construction and after evaluating the effects of refraction, see section V, flat non-focusing sub-mirrors were chosen. For this design, refraction at $n/n_{co} = 0.5$ is predicted to shift the antenna patterns such that the received power drops by <3dB. H-plane focusing is ruled out because of refraction but E-plane focusing is still under consideration and may be used in the future.

B. Bench and In-Vessel Microwave Tests

Bench measurements of individual waveguide components at 250GHz indicate the following: a) the WR28 straight sections have losses less than 0.3dB/m, b) the H-plane miter bends have between 1 and 2dB of loss each, c) the internal double 45° H-plane bend has ≈3dB of loss and d) the vacuum window interface has ≈2dB of loss.

Measurements of the H-plane antenna patterns, including the sub-mirrors indicated the following beam patterns: ≈14° for the -3dB full width (FW) and ≈20° for the -10dB FW points. These patterns result in a -3dB beam diameter of ≈16cm at the inside wall and ≈5.5cm at the bias ring. In addition, measurements of the free space transmission losses due to the spatial separation between launching and receiving antennas found -25dB for the 65cm single pass, inner leg system and -22dB for the 45cm double pass, outer leg system.

With the vacuum hardware installed in the DIII-D vessel, the total losses between the entrance and exit vacuum windows is measured to be -33dB for the inner divertor leg and -26dB for the outer divertor leg. The remaining external waveguide, miter bends and transition pieces will add another 4 to 6dB of loss per leg. Noting that the receiver has a measured noise floor of -65dBm, that the transmit power is about 0dBm (1mW) and allowing for a minimum signal to noise of 10 for the phase comparators, the expected dynamic range for the inner divertor leg system is ≈13dB (x20) and ≈20dB (x100) for the outer divertor leg.

V. Refractive and Vibration Effects

Refraction of the probe beam by density gradients is of concern for two reasons. First, the detected power may vary to the point that a phase measurement can not be made and second, the detected beam will take a bent path, accumulating a phase difference unrelated to the electron density. Figure 1 shows the wedge shaped geometry of the divertor leg which leads to two refractive effects. The first is from the oblique angle of incidence and the index of refraction change at the plasma interface, resulting in a neglectable deflection for $n/n_{co}<0.5$. The second results from the wedge shape which compresses the plasma producing a density gradient ∇n, oblique to the microwave beam path. Evaluating the phase change across the beam's diameter, we find:

$$\Delta\theta = (L_o/2\sqrt{\varepsilon})\ ((\nabla n)/n_{co}) \quad \text{radians}$$

where L_o is the path length through the plasma, $\varepsilon = (1-n/n_{co})$ is the dielectric constant and $n_{co}\approx 7.7e14/cm^3$ is the cutoff density.

As an estimate of this deflection we assume an average density of $n \approx 3.8e14/cm^3$ ($n/n_{CO}=0.5$) along the beam's center line, $\nabla n \approx 1.5e13/cm^4$ (outer leg) and $\nabla n \approx 0.5e13/cm^4$ (inner leg), and $L_o \approx 10cm$. These values produce $\Delta\theta \approx 4°$(outer leg) and $\Delta\theta \approx 1.5°$(inner leg), which will lead to a power reduction of ≈3dB or less for each leg. For either leg, the optical path length is increased by less than 0.3 fringes.

Mechanical vibrations are not expected to cause problems. Vibration data from the CO_2 interferometer indicates that the largest vessel motion of concern during normal operation is ≈0.01cm at ≈1Hz. This corresponds to ≈0.1 fringes which is neglectable compared to that expected by ELMs, ~1-5.

If vessel oscillations or strong refraction including cutoff due cause problems, then the two operating frequencies can be combined in one leg to act as a two color system, with the line average density determined by the phase difference between them. As a consequence, the resolution will be lowered and only one leg can be diagnosed.

Acknowledgments

The authors would like to acknowledge the valuable contributions of Dan Behne, Robert Childs, Ron Ellis, John Evans, John Doanne, Robert Geer, Don Hathaway, Brad Rice, John Smith, Barry Stallard, Craig Wendland and Reg Wood.

This work was performed under the auspices of the U.S. Department of Energy by the Lawrence Livermore National Laboratory under contract No. W-7405-Eng-48.

References:

1) 3D carbon composite is made by the Hercules Aerospace Company

2) Veron, D. Interferometery in Large Plasma Machines. In *Diagnostics for Fusion Reactor Conditions* (eds. Scott, P.E., Akulina, D.K., Leotta, G.G., Sindoni, E., and Wharton, C.) Vol.1 199. EUR 8351-1EN, CEC, Brussels (1982).

3) Hutchison, I.H. *Principles of plasma diagnostics*, pg. 87, Cambridge University Press (1987)

4) Hill, D.N., Futch, A.H., Leonard, A.W., Mahdavi, M.A., Petrie, T.W., et al., Journal of Nuclear Materials, Vol. 196-198, pg. 204 (1992)

5) McDonnell Douglas Test Report , EMTI Final Report #1165, August, 1989.

Figure captions:

1) Mechanical layout of the diagnostic. The Control Room Annex is located outside the experimental pit and the fiber optic run is ≈50m long. The scrape-off plasma flowing through the wedged shaped open field lines results in a ∇n oblique to the beam path.

2) Launching and receiving hardware in the V-1 port. All three mirrors are made of carbon. For the inside wall (not shown) the mirror is made of Inconel.

3) Thermal stress contours for (a) V-1 and (b) bias ring tiles. To improve the spatial resolution, only one half of each tile is assessed, but the boundary conditions on the righthand side are such as to simulate a full tile.

4) Microwave chassis schematic. Gunn diode outputs are ≈40mW and the tripled outputs are ≈1mW. The receiver has a noise floor of -65dBm. Log-linear amps provide an output signal proportional to each of the received 1mm signals.

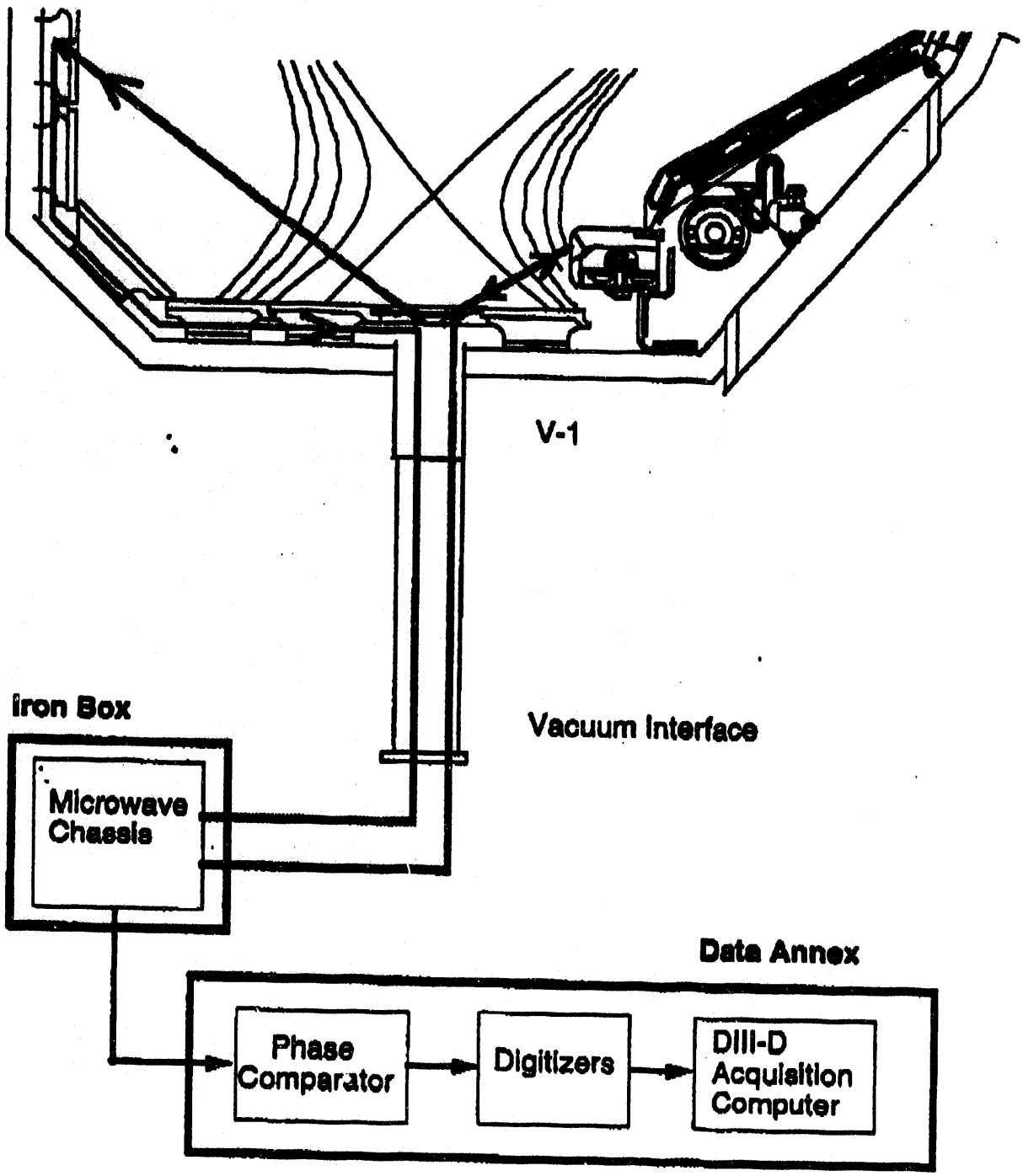
V-1
Iron Box
Vacuum Interface
Microwave Chassis
Data Annex
Phase Comparator
Digitizers
DIII-D Acquisition Computer

Figure 1.

Figure 2

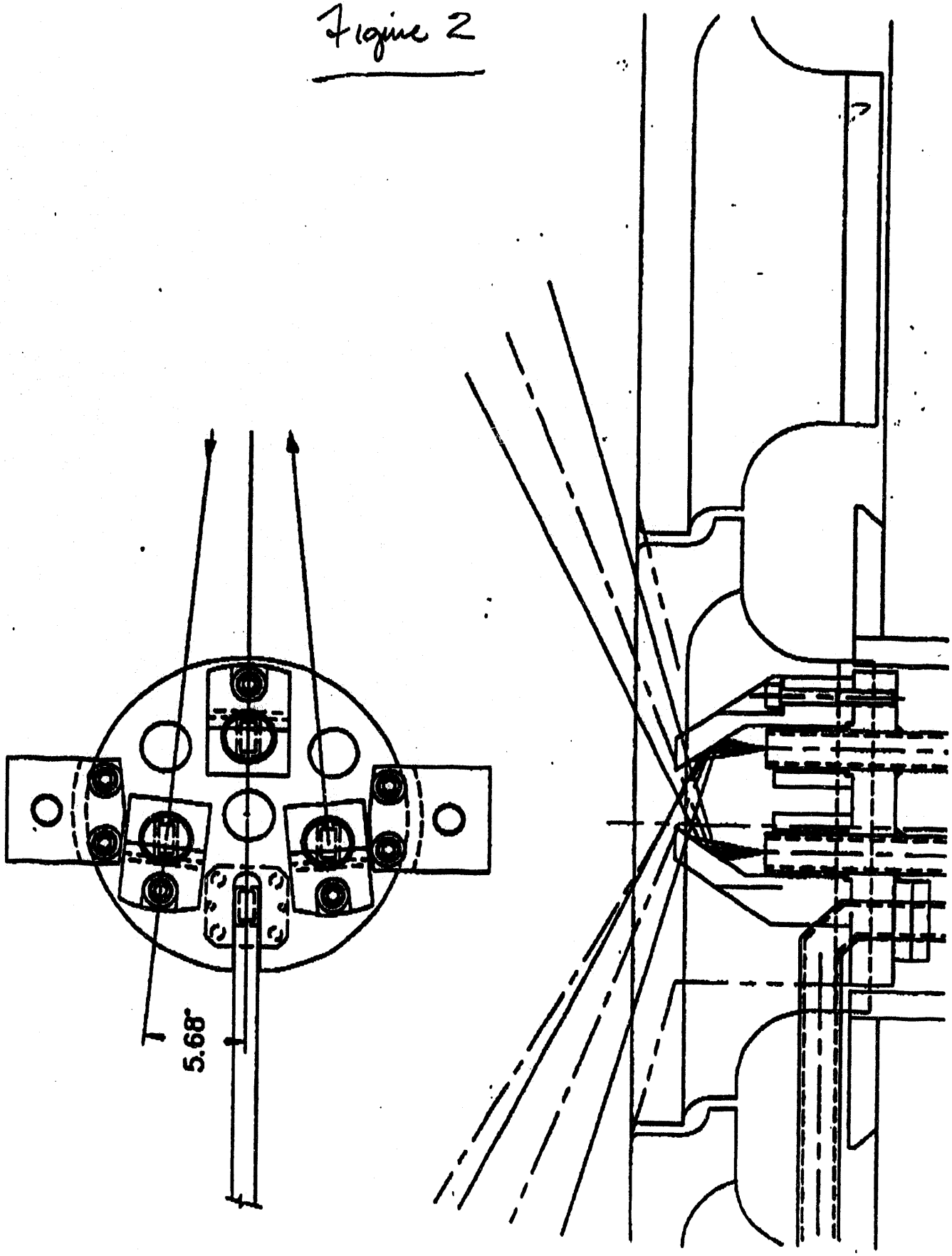

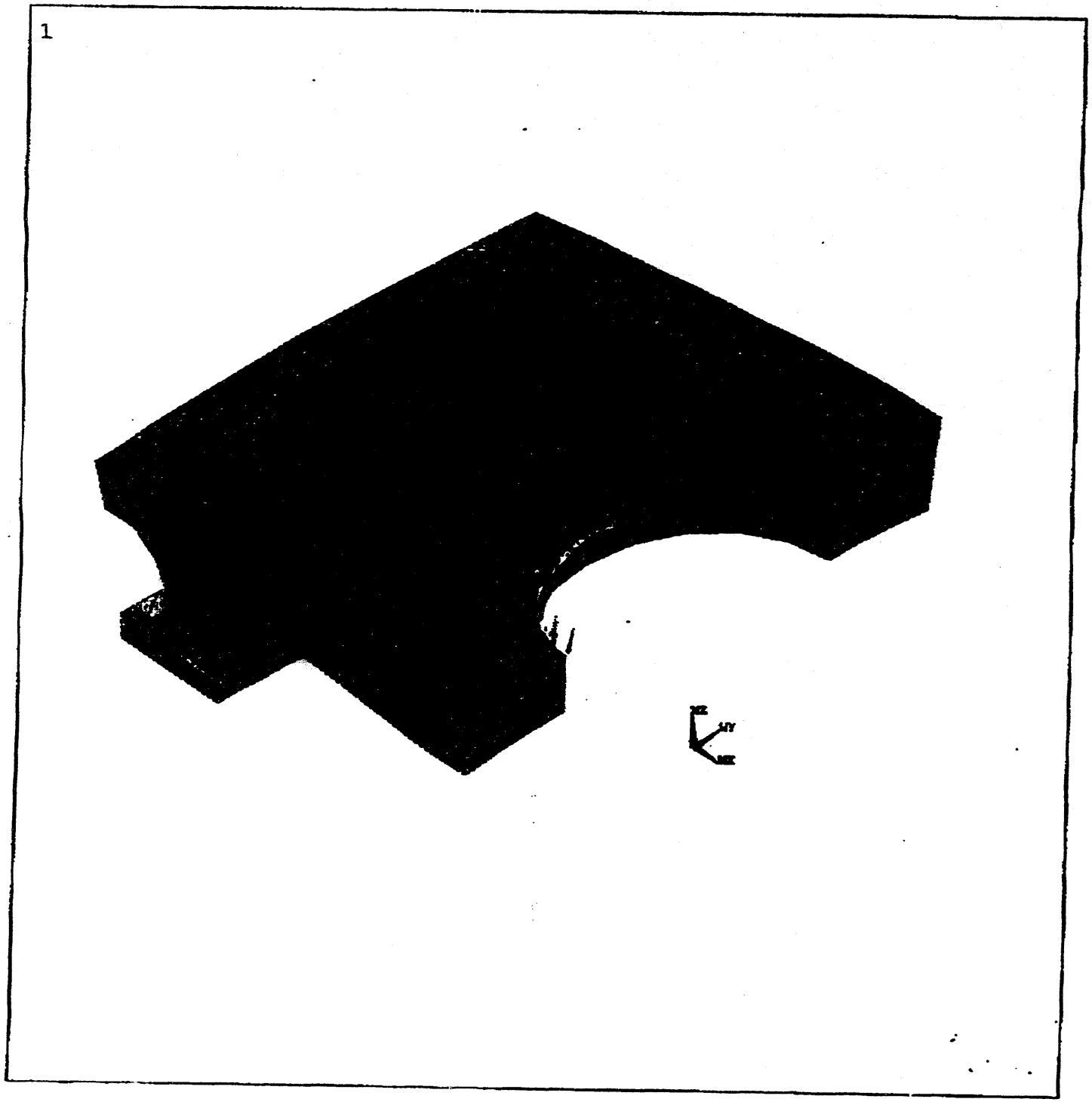
1
ANSYS 5.0 37
NOV 17 1993
09:47:43
PLOT NO. 1
ELEMENT SOLUTION
STEP=1
SUB =1
TIME=5
SZ (NOAVG)
RSYS=0
DMX =0.714E-04
SMN =-0.691E+08
SMNB=-0.782E+08
SMX =0.374E+08
SMXB=0.490E+08
HFLU
-0.691E+08
-0.573E+08
-0.454E+08
-0.336E+08
-0.218E+08
-0.993E+07
0.190E+07
0.137E+08
0.256E+08
0.374E+08

Figure 3a

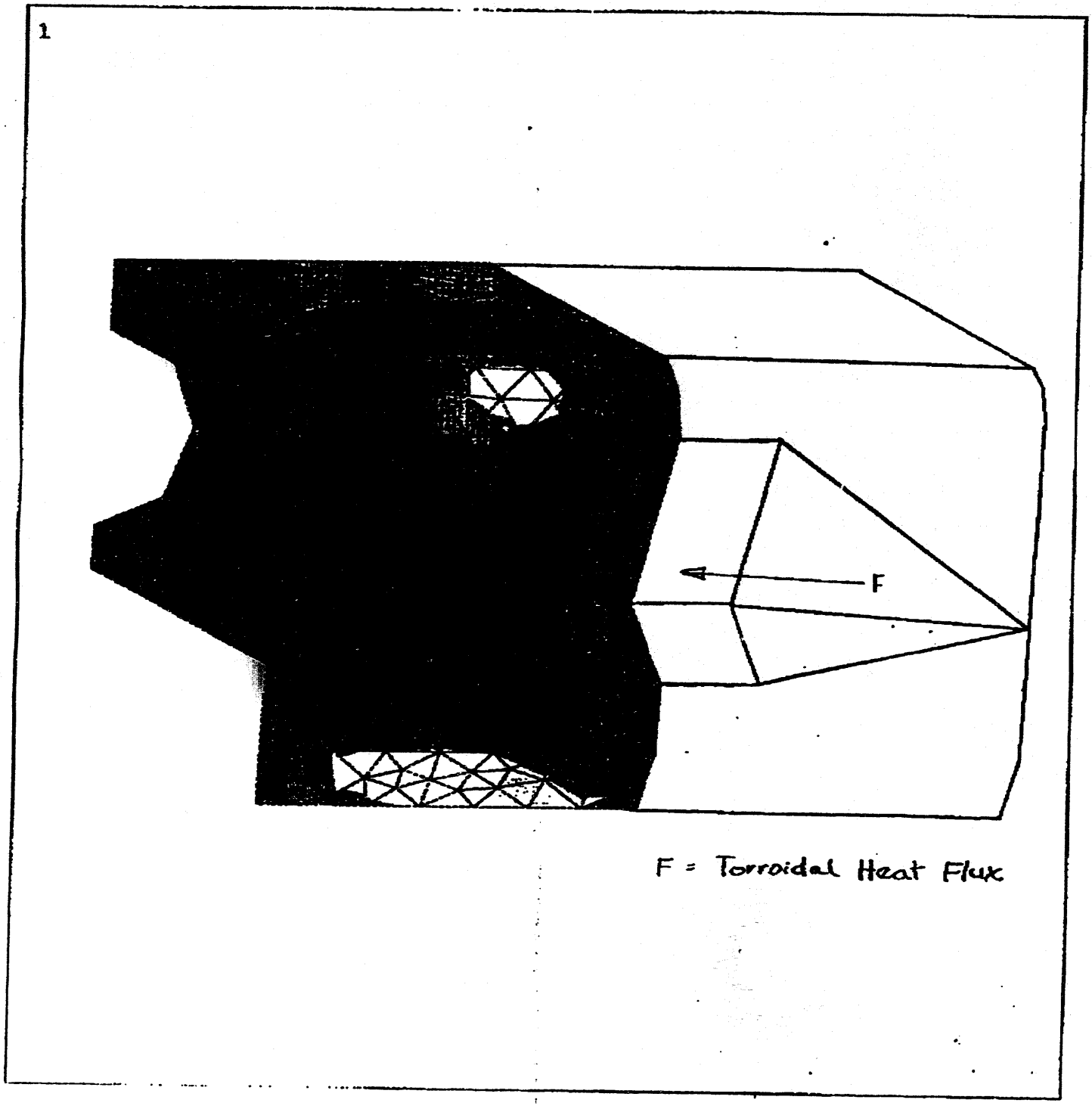

F = Toroidal Heat Flux

Figure 3b

250GHZ DUAL CHANNEL INTERFEROMETER

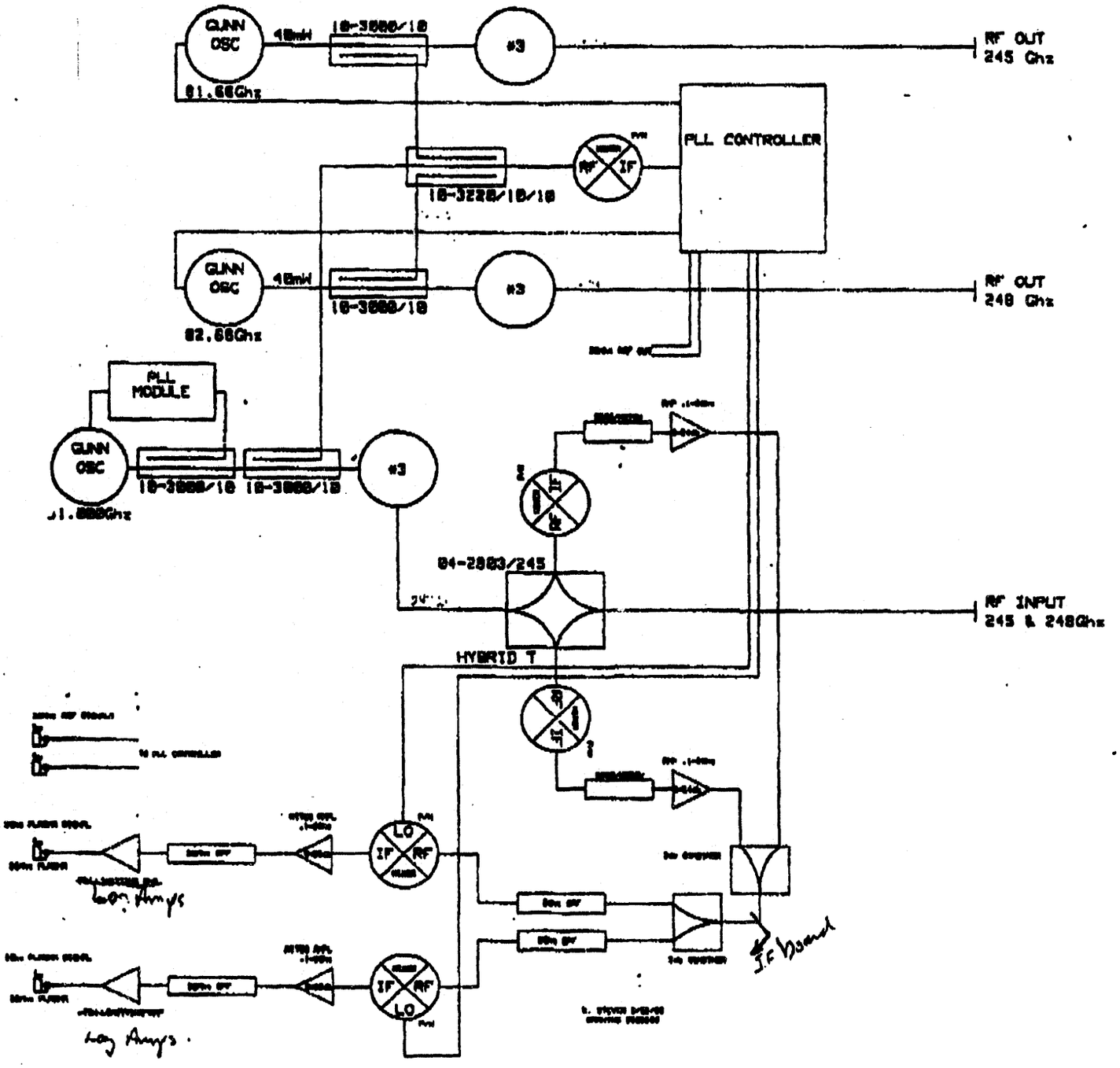

Fig. 4

DATE
FILMED
8/2/94

END